CHALMERS

UNIVERSITY OF TECHNOLOGY

Detailed Viscosity in Glycol Blends for Improved Spray Velocity Measurements

Detailed Density, Surface Tension and Viscosity at 20°C

Master Thesis

SERGI ROSELL BOCHACA

Department of Applied Mechanics
CHALMERS UNIVERSITY OF TECHNOLOGY
Gothenburg, Sweden 2016

Detailed Viscosity in Glycol Blends for Improved Spray Velocity Measurements

Detailed Density, Surface Tension and Viscosity at 20°C

SERGI ROSEL BOCHACA

Detailed Viscosity in Glycol Blends for Improved Spray Velocity Measurements
Detailed Density, Surface Tension and Viscosity at 20°C
Sergi Rosell

Cover: Left: Image of a spray obtained with a high speed camera; Right: Example of an image pair and it's respective velocity field obtained via PIV.

Detailed Viscosity in Glycol Blends for Improved Spray Velocity Measurements
Detailed Density, Surface Tension and Viscosity at 20°C
SERGI ROSELL BOCHACA
Department of Applied Mechanics
Chalmers University of Technology

Abstract

Knowledge and accurate prediction of physiochemical properties of liquid mixtures is of great importance for understanding intermolecular interactions—interactions which determine the macroscopic performance of liquid fuels used in modern high performance engines. Accurate prediction of viscosity and surface tension for binary mixtures of components with marked property differences remains a challenging task due to the nonlinearity and sensitivity of the detailed molecular interactions of the blend components. This challenge is compounded by the non-Newtonian fluid effects that begin to develop as seed-particles are added to the flow. For this work, detailed fluid measurements of viscosity, density, and surface tension were carried out using rigorously prepared binary mixtures of dipropylene glycol and water at nominal lab temperatures. In addition, a selection of 5 glycol/water blends were tested in the Chalmers steady spray rig under turbulent flow conditions. Here, microscale fluorescent particle velocimetry was applied to measure the internal velocity profile in a plain-orifice nozzle. These flows generated by the spray rig are central to several ongoing projects at Combustion, and highly sensitive to fluid properties. These data and the subsequent property model comparisons of this work directly support the primary breakup studies of the spray group at Combustion and studies of pulsating and constrained flows at Fluid Dynamics.

Acknowledgements

First of all, I would like to thank everybody who has encouraged me to undertake this adventure abroad.

Secondly, my sincere gratitude to Chalmers University of Technology, in particular to the Division of Combustion of the Applied Mechanics Department for the opportunity and support given. Also, I am extremly thankful to David Sedarsky, in particular for the chance of being part of a eye-opening project which can be usefull for future work at the department and other researchers.

Sometimes, as students,we do not always appreciate the amount of work behind all the tables filled with tons of values for the different substance properties. I was excited by the fact that this project permits a full experimental experience and allows me to understand the complexity of obtaining experimental data.

Third of all, I am deeply glad for all the support received from my family and friends from Spain, whom have always been there in case of unexpected events.

Last, but not least, thanks to all my Erasmus friends who, even during a motortrip through the deepest regions of Norway, have cheered me up on not giving up writing this Master Thesis report.

<div align="right">Sergi Rosell Bochaca, Gothenburg, June 2016</div>

Contents

Contents

Abbreviations

PIV   Particle Image Velocimetry
DPG   Dipropylene Glycol
H2O   Water
ST   Surface Tension
YST   Youngest Surface Tension
TK   Tamura and Kurata
MS   Myers and Scott
CW   Connors and Wright
RK   Redlich and Kister
SI   International System of Units
CGS   Centimetre-Gram-Second System of Units

List of Figures

List of Tables

List of Tables

1   Introduction

1.1   Project Motivation

This Master Thesis is part of a larger research effort for fundamental understanding of sprays, that is currently being carried out at Chalmers University of Technology, Department of Applied Mechanics, Division of Combustion.

The aim of the a number of projects at Applied Mechanics is to understand the physics underlying spray phenomena and provide solid tools and data to modellers to validate their work. In order to characterize he laboratory conditions, fluorescent particle seeded dipropylene glycol and water blends are used in a scaled spray rig to perform *Particle Image Velocimetry* analysis of the flow within the nozzle. With PIV it is possible to obtain the velocity profile of the flow through the nozzle.

Just velocity profiles are not enough boundary conditions, they must be accompanied with the respective properties, such as density, surface tension and viscosity, of the fluid that is being studied in order to provide inputs for CFD modeling of spray phenomena. There is a lack of relevant data in the literature.

In addition, PIV analysis of five well-known dipropylene glycol and water blends was undertaken in support of this work. A description of this analysis can be found in the appendix C.

1.2   Objectives

The targets set for the current project are the following:

1. Obtain detailed density, surface tension and viscosity curves for differerent dipropylene glycol and water blends at laboratory temperature.

2. Verify the experimental data trends by means of tested empirical correlation models.

3. Publish a journal article sharing the detailed property measurements and error analysis.

1.3   Methodology

In order to achieve the targets proposed for this particular project the next methodology has been followed.

In first place, a literature review has been performed in order to aquire data for comparison of the different properties of interest (density, surface tension, viscos-

Table 1.1: Composition of the used blends in volume fraction.

	%DPG	%H2O
1	100	0
2	95	5
3	90	10
4	85	15
5	80	20
6	75	25
7	70	30
8	65	35
9	60	40
10	55	45
11	50	50
12	45	55
13	40	60
14	35	65
15	30	70
16	25	75
17	20	80
18	15	85
19	10	90
20	5	95
21	0	100

ity). Besides theoretical aspects of fluid properties, this literature review includes a revision of the measurement methods that have been used for testing the blends, as well as an explanation of some empirical correlation methods which are of interest for a subsequent data analysis and validation.

Those empirical models are needed because there are no theoretical models that accurately estimate the liquid mixtures viscosity without a previous correlation with experimental data in most cases. Also, each single model is only valid in a limited range of conditions.

Twenty one liquid mixtures have been prepared prepared. The table 1.1 compiles the composition of the blends.

These blends have been subjected to three different tests in order to obtain experimental data for the fluid properties of interest. Several runs for each experimenthave been performed in order to reduce the uncertainty to manageable levels.

Finally, the data have been correlated with appropiate methods identified in the literatures study.

2 Theoretical Background

The goal of the following chapter is to provide basic information on the of fluid properties and liquid mixtures for a better understanding of the results which will be discussed in further chapters.

2.1 Liquid Mixtures Properties

For prediction of fluid properties and behaviour, the *ideal mixture* approximation is widely considered. In this simplified regime resulting blend behavior is analogous to ideal gases, but with liquids it is not possible to neglect the molecular interactions. Instead of this, it is assumed that all the interactions between the molecules of the mixture have the same mean strength. Basically, it means that volumes are strictly additive, ideal solutions are always miscible and thermodynamic attributes can be calculated as apparent molar properties (molar average), z_m:

$$z_m = \sum_{i=1}^{n} x_i z_i \tag{2.1}$$

Where z_m is the property of the mixture, x the molar fraction, z corresponds to the property of the pure liquid, n the number of species in the mixture, and the subindexes i, m denote the component and the mixture, respectively.

However, this is valid only when assuming that the molecular interactions are equal between the fluid molecules, which normally is not the case. Consequently, the behavior tends to be nonideal for real mixtures. To express that nature the excess molar quantities are used.

Excess molar quantities, Δz, are defined as the difference between the partial molar property measured in a real mixture and the value of the property in an ideal mixture:

$$\Delta z = z - \sum_{i=1}^{n} x_i z_i \tag{2.2}$$

2.2 Density

Density, ρ, can be easly understood as the relation between the mass per unit volume of a substance.

$$\rho = \frac{m}{V} \tag{2.3}$$

Where m is the mass and V is the volume of the substance.

There are a number of reliable methods to determine the density of liquids. One simple method, which was used in this project, is to weigh a determined quantity of the fluid, such that the known mass and volume can be used to obtain the density

using equation 2.3.

In the international system of units (SI) density is expressed in kg/m^3. In the centimetre-gram-second system of units (CGS) the unit is g/cm^{-3}.

2.3 Surface Tension

Surface tension, σ, is a property of a fluid surface that makes it tend to acquire the least surface area possible. This phenomena is caused by the cohesive forces among liquid molecules. Within the fluid, every single molecule is subjected to the same forces, resulting in a force equilibrium. However, at the surface (for example, at a liquid-air interface), this force equilibrium is not zero, since they do not have the same molecules on all sides. This non-equilibrium causes an internal pressure that tries to contract the fluid to the minimal area possible, simultaneously creating a surface layer. A clear example of that layer is that small insects, such as water striders, can walk on water because they are not heavy enough to break the surface tension of water.

This surface tension effect can be expressed with the Young-Laplace equation formulation for a sphere, equation 2.4, and taking into account that all the systems always try to achieve a minimum potential energy state, a fluid droplet will naturally conform to a spherical geometry obtaining the least surface area per volume unit:

$$p = \frac{2\sigma}{r} \tag{2.4}$$

Where p is the pressure, σ represents the surface tension, and r the radius of the sphere.

For pure liquids molecular interactions remain constant in time, insomuch as the molecules always have the same neighbours. But when some impurities or fluids are mixed, this molecular arrangement can vary over time. Figure 2.1 shows this effect.
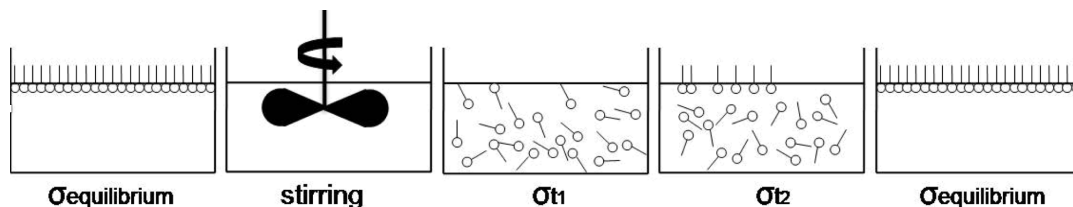
Figure 2.1: Schematic evolution of the molecular organization in the fluid after stirring.

When the fluid mixture is steady, surface tension remains constant (also called *equilibrium surface tension*). In this state, molecular movement can be considered null so the force equilibrium does not change. If a pertubation is applied, the molecular equilibrium is broken and the value of the surface tension changes because of the

instability of the system.

If the liquid mixture is allowed to stand until it reaches a static state, surface tension will gradually decrease achieving equilibrium value. An example is given in the figure 2.2, where for tap water the surface tension value does not have major changes in time whereas for a randomly chosen blend varies over time.
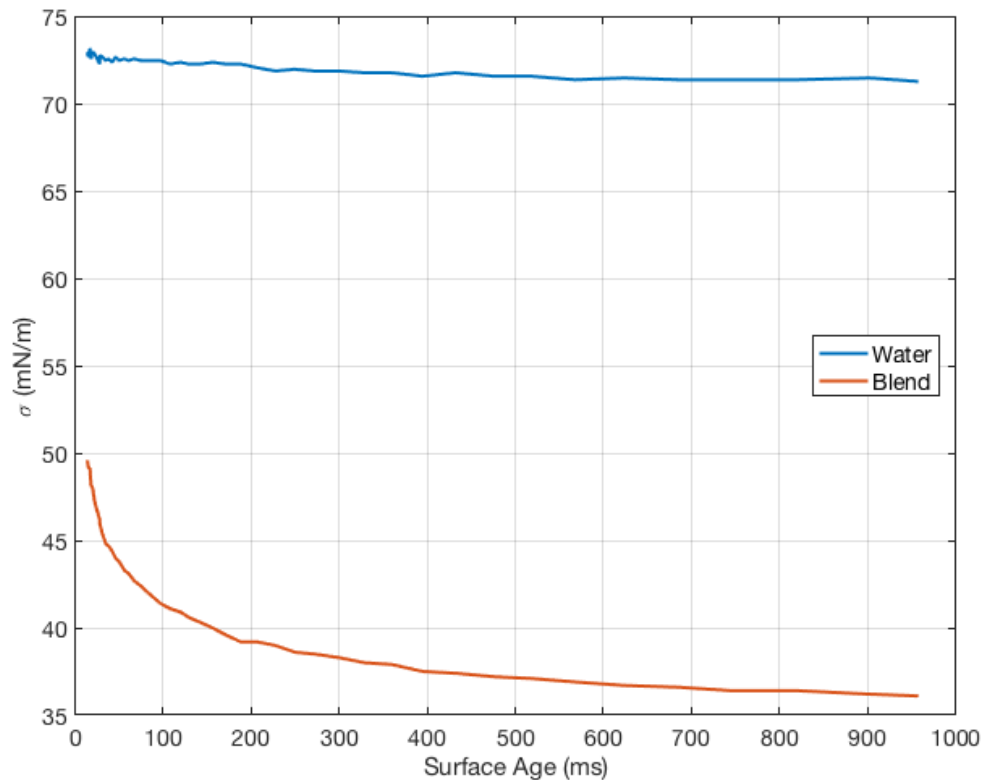
Figure 2.2: Evolution of surface tension of water and a random selected blend at 20 °C measured at the laboratory.

Therefore, *dynamic surface tension* is defined as the value of the surface tension at a particular surface age. It is crucial when simulating and modelling processes where interfaces are produced extremly quickly such as spraying, foaming, emulsifying, coating, etcetera... So the appropiate value of the surface tension for these applications the *youngest surface tension*.

In the SI units system, the unit of surface tension is N/m.

2.3.1 Bubble Pressure Tensiometer

Bubble pressure tensiometers are devices that use the bubble pressure method for determining the dynamic surface tension of a fluid. Essentially, the maximum internal pressure of an air bubble that is formed in a liquid sample via a capillary is measured.

$$r_1 > r_2 > r_3 = r_c < r_4 < r_5 \tag{2.5}$$
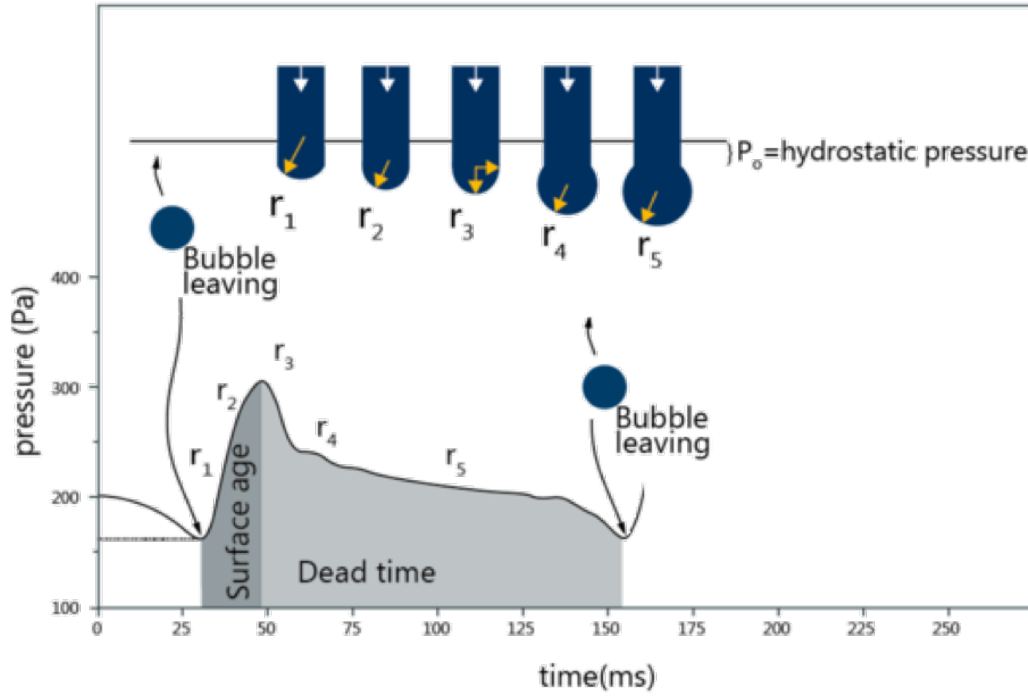
Figure 2.3: Schematic representation of the bubble formation and its effect on the measured pressure.

As shown in the figure 2.3, a gas bubble is produced at the tip of the capillary. The bubble radius initially increases and then decreases giving rise to a pressure maximum when the radius of the bubble coincides with the capillary radius.

The period of time from the beginning of the interface formation, or bubble production, to the moment of the measurement, when the maximum pressure is reached, is defined as the *surface age*. It is possible to calculate the dependency of the surface tension over time by varying the speed at which bubbles are created.

Finally, making use of the Young-Laplace equation it is possible to calculate the surface tension of those air bubbles produced within the sample. Manipulating the equation 2.4:

$$\sigma = \frac{1}{2}(p_{max} - p_0)r_c \tag{2.6}$$

Where p_{max} is the maximum pressure measured during the formation of the bubble, p_0 denotes the hydrostatic pressure due to the capillary immersion and the liquid density, and r_c the capillary radius.

2.3.2 Correlation and Estimation of Surface Tension

The simplest method of estimating surface tension of binary liquid mixtures is presented in the equation 2.1, just a molar combination of the pure liquids surface tension value. However, it has been found that the surface tensions deviates significatively from this linear function. This character can be explained by the fact that there is a migration of the component with lower surface tension molecules to the surface layer, thus minimazing the Helmholtz free energy of the mixture.

To reiterate, the surface tension of a liquid mixture is not only a function of the surface tensions of the pure liquids. It depends on the composition of the bulk phase and the composition at the vapor-liquid interface, the temperature of the system, the migration of molecules, the free energy per unit of area, etcetera... There are some complex theoretical methods [1–5], which attemp to account for the effect of the bulk composition. In order to do so, they use properties such as the density or parachors [6], and those are not available.

Therefore, theoretical estimations are of limited use for this project because the density of the mixtures are unknown. However, there are several approaches for estimating the surface tension of mixtures based on empirical or semi-empirical thermodynamic and statistical mechanical grounds.

Connors and Wright [7] proposed an equation relating the surface tension to the composition of binary aqueous solutions, making use of thermodynamical and statistical mechanics methods. Giving fairly accurate results in the chemical literature [8]:

$$\sigma = \sigma_1 - \left[a + \frac{bx_1}{1 - ax_1}\right] x_2(\sigma_2 - \sigma_1) \tag{2.7}$$

Where a and b are adjustable parameters to be determined with experimental data.

Fu et al. [9] proposed the following equation based on a modified Hildebrand-Scott equation for binary systems:

$$\sigma = \frac{x_1\sigma_1}{x_1 + x_2 f_{12}} + \frac{x_2\sigma_2}{x_2 + x_1 f_{21}} - \frac{x_1 x_2 |\sigma_1 - \sigma_1|}{(x_1 + x_2 f_{12})(x_2 + x_1 f_{21})} \tag{2.8}$$

Where f_{12} and f_{21} are adjustable coeficients.

As mentioned earlier, it is possible to quantify the deviation from the ideal behavior of the mixture by using excess surface tension, $\Delta\sigma$:

$$\Delta\sigma = \sigma - \sum_{i=1}^{n} x_i\sigma_i \tag{2.9}$$

The following formulae introduce tested empirical models for excess surface tension calculations using experimental data for binary systems:

1. Edited Redlich-Kister equation by Mosteiro [10]:

$$\Delta\sigma = x_1 x_2 \sum_{p=0}^{p=m} A_p(x_1 - x_2)^p + B_0(x_1 - x_2) \tag{2.10}$$

Where A_p and B_0 are the adjustable parameters, and m the number of parameters to be determined.

2. A simpler equation proposed by Santos et al. [11]:

$$\Delta\sigma = x_1 x_2 (A + B[1 - (x_1 - x_2)]^C) \tag{2.11}$$

Where A, B and C are adjustable parameters.

3. A rational expression suggested by Myers and Scott [12]:

$$\Delta\sigma = x_1 x_2 \left(\frac{\sum\limits_{p=0}^{p=m} B_p(x_1 - x_2)^p}{1 + \sum\limits_{l=0}^{l=m} C_l(x_1 - x_2)^l} \right) \tag{2.12}$$

Where B_p and C_l are adjustable parameters.

In general, these excess surface tension correlation models are more accurate than the theoretical models, however they have more adjustable parameters. All the models shown here are for equilibrium surface tension. The literature survey failed to turn up any dynamic surfacce tension correlation models.

2.4 Viscosity

As surface tension, viscosity is also a fundamental property of all fluids. It can be understood as a measure of the resistence of the fluid to flow or shear. Generally, viscosity is expressed in one of in two forms [13]:

1. Absolute or dynamic viscosity, μ: Tangential force per unit area required to move one horizontal plane with respect to an other plane, at an unit velocity while maintaining an unit distance between planes. It relates the shear stress, τ, with the shear rate, $\dot{e}$:

$$\tau = \mu\dot{e} \tag{2.13}$$

In the SI units system, the unit of dynamic viscosity is $Pa \cdot s$. In the CGS system, the unit used is the *Poise*.

2. Kinematic viscosity, ν: Ratio of dynamic viscosity and density. Represents the same characteristic as the dynamic discarding the effect of the forces that generate the flow.

$$\nu = \frac{\mu}{\rho} \tag{2.14}$$

In the SI units system, the unit of kinematic viscosity is $m^2 \cdot s$ or *Stoke*.

Additionally, viscosity is used as a fluid classification system, dividing them in two catergories:

1. Newtonian: Fluids in which viscosity is constant at any shear rate, stress and time. Meaning that shear stress is always proportional to shear rate.

2. Non-Newtonian: Roughly, fluids with a non-constant viscosity. There are two types of non-Newtonian fluids: time dependent (change in viscosity with time under conditions of constant shear rate) and time independentent (viscosity varies as shear stress varies).

2.4.1 Rotational Viscometers: Coaxial-Cylinder

Rotational viscometers are devices that operates on the principle of measuring the rate of rotation of a solid in a viscous medium upon application of a known force or torque required to rotate the solid shape at a definite angular velocity. Basically, the main difference between the different types of rotational viscometer is in the spindle design. For this project a cylindrical spindle has been used for carrying out the measurements.

Figure 2.4 shows a basic design of a coaxial-cylinder rotational viscometer. It consists of a steady outer cylinder that contains the fluid sample and of a suspended inner cylinder that is rotated at a constant speed. As a result, a torque is measured by the angular deflection of the inner cylinder. It is possible to vary the velocity of rotation to obtain data on the change in viscosity of the fluid with the shear rate. this facilitates working with both newtonian and non-newtonian fluids.

Knowing the geometric parameters of the viscometer, C, the speed of rotation, Ω, and measuring the torque, T, the dynamic viscosity of the fluid may be calculated from the equation 2.15. The geometric parameters are described in figure 2.4.

The constant C is particular for every viscometer and needs to be adjusted during the calibration process of the instrument as it does not take into account the forces at the end of the cylinder. Nevertheless, once the device is well calibrated, it is capable of determining viscosities over the range of 0.01 to 100 poise in various working conditions.

$$T = \frac{4\pi R_1^2 R_2^2 h \mu \Omega}{R_1^2 - R_2^2} = C\mu\Omega \tag{2.15}$$
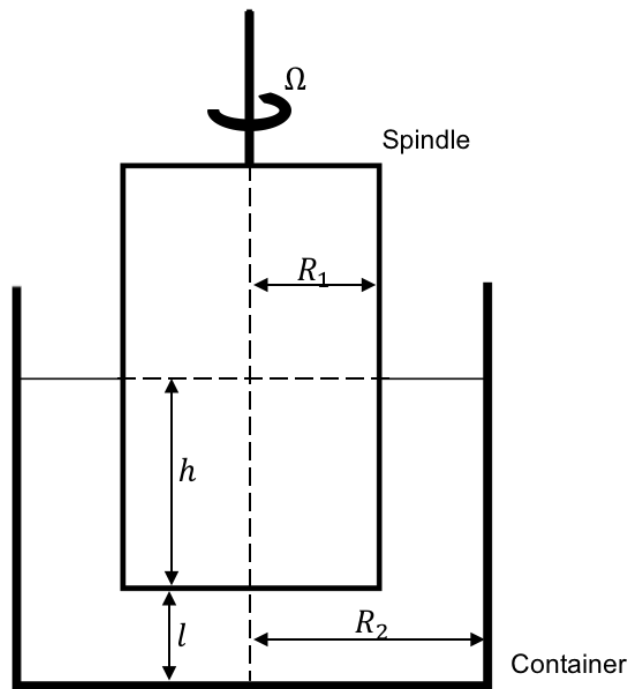
Figure 2.4: Sketch of the a coaxial-cylinder rotational viscometer detailing the geometrical parameters.

2.4.2 Correlation and Estimation of Liquids Viscosity

At the moment there is no universal theory which would allow exact calculation of viscosity of a complex mixture from the viscosities of the individual components [19]. In this subsection two different approaches to estimate liquids mixture viscosity are followed [13, 14]:

1. Extension of pure liquids viscosity estimation methods to mixtures by means of semi-theoretical equations.

2. Application of mixtures rules to pure component viscosity models based on theory and/or experimental data.

Like most fluid properties, expecting the mixture viscosity to be a linear function of composition (molar, mass, volume) is normally not accurate, not even for liquid mixtures which are nearly ideal. Usually, an exponential type of dependence is observed mostly in liquids with a larger difference in viscosity. The following list mentions empirical methods that can be used in some situations to estimate the viscosity of a liquid mixture:

1. Additive models, providing good precision for ideal mixtures:

$$f(\mu) = \sum_{i=1}^{n} x_i f(\mu_i) \tag{2.16}$$

Where:

$$f(\mu) = \mu \quad \text{or} \quad \ln(\mu) \quad \text{or} \quad \mu^{-1} \tag{2.17}$$

2. Kendall and Monroe proosed an equation that has low theoretical substantiation and does not give satisfactory accuracy for most cases:

$$\mu^{1/3} = x_1 \mu_1^{1/3} + x_2 \mu_2^{1/3} \tag{2.18}$$

3. Arrhenius recommended, also an additive model that is perfectly followed by ideal mixtures. This theory can be understood within the framework of the absolute rate theory:

$$\log(\mu) = x_1 \log(\mu_1) + x_2 \log(\mu_2) \tag{2.19}$$

It has been reported that for the last two models to be applicable, the two components of the mixture need to have a similar structure, be non-polar and non-associated or one of them should dominant in quantity. Furthermore, the difference in viscosity of the two components should be smaller than 15 $Pa \cdot s$.

4. Irving suggested a one parameter Grunberg-Nissan formula, has given good results for a widely range of multicomponent mixtures, except for aqueous solutions. For binary mixtures:

$$\log(\mu) = x_1 \log(\mu_1) + x_2 \log(\mu_2) + x_1 x_2 d \tag{2.20}$$

Where d is a molecular interaction parameter dependent on temperature but independent of composition. It includes the non-ideality behavior of the system. Meaning that is linked to the fact the interaction energy between two unlike molecules is in general different from the interaction energy of two like molecules. Also, it can be calculated with a single data point.

5. A modification to the Grunberg-Nissan equation has been proposed by Oswal and Desai, who added two additional parameters:

$$\log(\mu) = x_1 \log(\mu_1) + x_2 \log(\mu_2) + x_1 x_2 d + K_1 x_1 x_2 (x_1 - x_2) + K_2 x_1 x_2 (x_1 - x_2)^2 \tag{2.21}$$

Where K_1 and K_2 are adjustable parameters with no physical meaning.

6. Van der Wyk relation:

$$\ln(\mu) = x_1^2 \ln\left(\frac{\mu_1 \mu_2}{\mu_{12}}\right) + 2x_1 \ln\left(\frac{\mu_{12}}{\mu_2}\right) + \ln(\mu_2) \tag{2.22}$$

Where μ_{12} is a interaction coeficient, same as the coeficient d in the equation 2.20.

7. Tamura and Kurata [15] proposed the following model:

$$\mu = x_1 v_1 \mu_1 + x_2 v_2 \mu_2 + 2\mu_{12}(x_1 x_2 v_1 v_2)^{1/2} \tag{2.23}$$

Where v is the volume fraction of the components and μ_{12} denotes the adjustable parameter with the same meaning as the two anterior models.

The model is suitable for estimating viscosity of nonpolar - polar, polar - polar and nonpolar - nonpolar mixtures with an average error of 5 to 7%.

8. There are more complex models, such as Lima's form of Souders' equation:

$$\log(\log(10\mu)) = \rho \left[\frac{(x_1 I_1 + x_2 I_2)}{(x_1 M_1 + x_2 M_2)} \right] - 2.9 \tag{2.24}$$

Where M is the molar mass of the components and I represents viscosity constants calculated from the atomic and structural contributions. If there is no viscosity data, the Rheochor method can be used as a guess for the viscosity values. The model has an average deviation of 12% for nonpolar and slightly polar mixtures.

9. The Lederer and Roegiers equation, a single parameter model that also takes into account the difference in intermolecular cohesion energies between the components:

$$\ln(\mu) = \ln(\mu_1) + \frac{\alpha x_2}{x_1 + \alpha x_2}(\ln(\mu_2) - \ln(\mu_1)) \tag{2.25}$$

There are models in the literature to estimate viscosity of mixtures by means of kinematic viscosity, such as McAllister:

$$\ln(\nu) = x_1^3 \ln(\nu_1) + 3x_1^2 \ln(\nu_{12}) + 3x_1 \ln(\nu_{21}) + x_2^3 \ln(\nu_2) - \ln\left(x_1 + x_2 \frac{M_1}{M_2}\right)$$
$$+ 3x_1^2 x_2 \ln\left(\frac{2 + M_2/M_1}{3}\right) + 3x_2^2 x_1 \ln\left(\frac{1 + M_2/M_1}{3}\right) + x_2^3 \ln\left(\frac{M2}{M_1}\right) \tag{2.26}$$

Where ν is the kinematic viscosity, ν_{12} and ν_{21} are interaction parameters that can be determined from two data points.

The models that have given best results in the chemical literature, from a theoretical point of view are Grunberg-Nissan, Tamura and Kurata and Lederer and Roegiers.

Finally, excess molar properties can also be used for viscosity:

$$\Delta\mu = \mu - \sum_{i=1}^{n} x_i \mu_i \tag{2.27}$$

The excess viscosity can be correlated by means of Redlich-Kister equation [8]:

$$\Delta\mu = x_1 x_2 \sum_{p=0}^{p=m} A_p (x_1 - x_2)^p \tag{2.28}$$

Where A_p are the adjustable parameters, and m the number of parameters to be determined.

2.5 Data for DPG and H2O Mixtures from Sun et al.

The table 2.1 lists the data for water, dipropylene glycol and its blends at 25, 50 and 75% DPG molar fraction composition. The extent of this data is remarkably short. Surface tension data is not available for the mixtures. In addition, the values are not given at the same temperature which hinders useful interpolation of the properties [16, 17].

Table 2.1: Density and viscosity for DPG(1) + H2O blends at approximately 20 °C.

		H_2O	$x_1 = 0.25$	$x_1 = 0.50$	$x_1 = 0.75$	DPG
T	[K]	293.15	295.05	293.40	293.90	293.15
ρ	[kg/m^3]	998.20	1,040.00	1,034.00	1,028.00	1020.60
μ	[mPa·s]	1.01	22.30	59.90	88.50	100.00
σ^1	[mN/m]	72.80	-	-	-	35.00^2

Data for pure DPG depends in part on the details of the production process, used by the manufacturer. Also, glycols degrade slowly in the presence of oxygen, in addition, DPS is sensitive to UV light, which can act as a radical initiator and initiate oxidation reactions. Those reactions can be speed up if the liquid is not stored properly.

In the case of the DPG used during the experiments the manufacturer does not include information regarding surface tension.

---

[1]equilibrium surface tension.
[2]at 25 °C or 298.15 K.

3 Experimental procedure

As explained in previous sections, the goal of this project is to obtain detailed curves for three fluid properties: density, surface tension and viscosity. For this purpose, the following experiments have been carried out in order to obtained the desired data.

It is important to guarantee the quality and precision of the experimental data. In order to do so and for the sake of the experiments, during the next sections the accuracy, calibration method, experimental procedure are described.

3.1 DPG + H2O mixtures

Dipropylene Glycol consists of a mixture of three isomeric chemical compounts, 4-oxa-2-6heptandiol, 2-(2-hydroxy-propoxy)-propan-1-ol, and 2-(2-hydroxy-1-methyl-ethoxy)-propan-1-ol. There can be other minor organic compounds as a result of the manufacturing process, normally corresponding to a mass fraction less than 1%. Its molar mass is 134.73 g/mol.

Apart from the fluid properties mentioned in the table 2.1, DGP is miscible in water, which means that it forms a homogenous mixture when added together. The hydroxyl groups present in the molecules that make up the liquid give it its polar character. Also, it is colorless, making it suitable for optical use, odorless, has low-toxicitym and a newtonian behavior.

This compound is mainly used as a plasticizer, as a polymerization initiator, as a monomer, as intermediate in some industrial chemical reactions, as a solvent (for example in perfumes, and skin and hair care products).

The material, *Dipropylene Glycol (99%) Mixture of Isomers*, was used as delivered by *SIGMA-ALDRICH*.
Water the most common fluid on earth. It is a newtonian, polar, transparent fluid considered a universal solvent, with molar mass is 18.01528 g/mol. If mixed with DPG, the result is a liquid with newtonian character, odorless, colorless, polar.

The main reason to use tap water instead of deonized is that the mixtures that are being currently used in the spray rig contain tap water. Tap water has been used to prepare the blends after testing its properties.

3.2 Blend Preparation

As said in section *1.3*, 21 different dipropylene glycol and water blends have been studied. Taking into account that the blend number 1 and 21 correpond to the pure

liquids, so there are ninteen mixtures that have been prepared.

Due to the strong wetting effect exhibited by DPG, the liquid mixtures have been prepared by mass using an electronic balance FX-300 AND [18], figure 3.1. The device employed has a precision of 0.00229 g, calculated in the appendix A. The accuracy calculation is explained in the appendix *B*, and the real blend composition and error is discussed in the following section *4.1*.

Figure 3.1: Electronic balance, FX-300 AND, used for blend preparation and dentisty determination.

3.3   Density Calculation

The method applied for determining the density iof the fluid blends was covered in the theoretical background of this report, section *2.2*. Using the same balance detailed above, a known volume of liquid mixture has been measured.

EXTEND

3.4   Bubble Pressure Test

Figure 3.2 shows the bubble pressure tensiometer BP50 by KRÜSS [19] that has been used to carry out the dynamic surface tension measurements. The device has been calibrated with deionized water at 20 °C. The accuracy of the surface tension measurement is 0.05 mN/m, and 0.05 °C for the temperature.

Figure 3.2: KRÜSS Bubble pressure tensiometer BP50 used for surface tension measurements.

3.5 Viscosity Determination

Dynamic viscosity has been measured in order to reduce the error propagation in the measurements, since density is unknown and is being measured. In case of testing kinematic viscosity an extra doubt would be introduced in the data.

A rotational viscometer for low viscosity, DV2T Brookfield LV, figure 3.3 with an ultra low velocity spindle, ULA spindle, figure 3.4, has been used for obtaining viscosity data. The device is new, then no calibration was needed because it was guaranteed by Brookfield. The accuracy in viscosity measurement, e_μ, is described by the equation 3.1, representing the 1% of the full scale of viscosity range. This equation is particular for every spindle and device.

$$e_\mu = \frac{6}{\Omega} \tag{3.1}$$

As the resulting mixture of two newtonian liquids is another newtonian fluid, the test was performed with a constant angular velocity during a time interval. In order to select the correct angular velocity to perform the experiment, as well as validate the data, 2 criteria recommended by Brookfield have been followed [20]:

1. Torque value measured has to be between 10 and 100% of the dynamic range of the sensor. This depends on the angular velocity at which the device is

operating.

2. A laminar regime must be ensured. If a turbulent flow is reached, it might drived a non-linear increase of the viscosity value. To assure that for this particular set up, the ratio between the angular velocity and the viscosity must not surpass 82.35. This value is provided by the manufacturer and is just valid for this geometry and spindle.

Figure 3.3: DV2T Brookfield LV viscometer.

Figure 3.4: Ultra low viscosity spindle used in the viscosity test.

4   Results and Analysis

This chapterdiscusses the results obtained. The methodology followed for the analysis of the surface tension and viscosity data is the following, density is treated differently: first, it is shown a dotgraph to represent the number of experiment runs and how the results are distributed. Secondly, an errorgraph with an empirical correlation of the experimental data, and finally the correlation of the excess molar property. Finally, a comparison between models has been made.

Auxiliar calculations needed, as well as the averaged experimental data can be found at the appendix A and B.

4.1   DPG + H2O Blending Results

Even though it is possible to try to be as precise as conceivable, even when you are careful there is some error, so it is impossible to achieve the theoretical composition value desired for the blends. The figure 4.1 shows the difference between the real and the theoretical volume fraction for the liquid mixtures. The real values obtained for the compositions, in volume and molar fraction, are displayed in the table B.2. Blends number 1 and 21 are not considered since they represent the pure liquids.
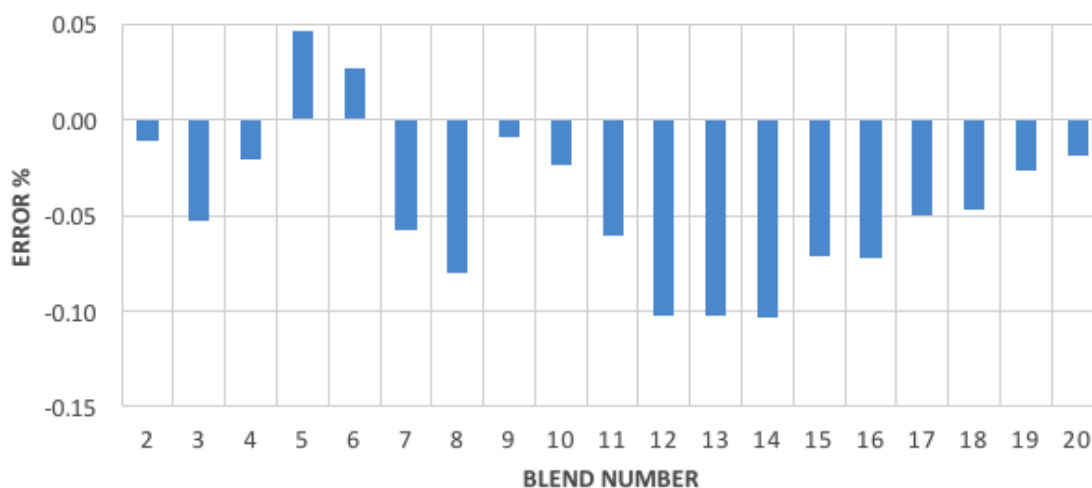

Figure 4.1: Difference between the real DPG volume fraction and the theoretical DPG volume fraction achieved.

The maximum difference between the real and theoretical volume fraction is around the 0.11%. Also the maximum uncertainty for the blends is below 1%. The blends are well prepared for the purposes of these measurements because of the low uncertainties achieved.

4.2 Density

As can be seen in the figure 4.2, density data is quite homogeneously distributed. 4 data prints were taken for every blend due to the time cost of the experiment, and the accuracy of the instruments used. However, the experiment was precies enough to demonstrate the non-ideal behavior of the mixtures.
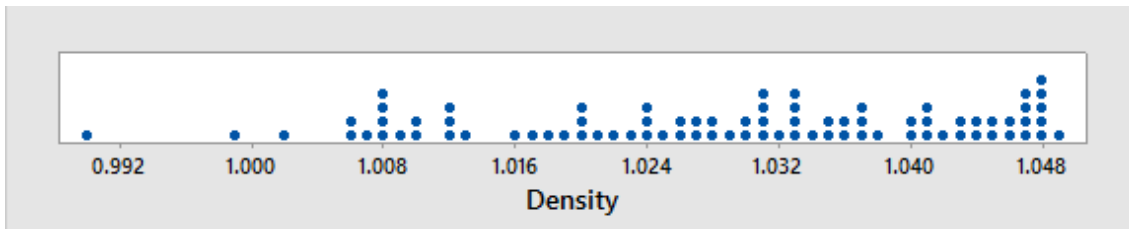
Figure 4.2: Density experimental data distribution. One dot can represent up to 5 points.

For this reason, instead of using the excess molar volume to correlate the results, a 4_{th} order polynomial fitting has been applied, equation 4.1. Thus obtaining the coefficients and sum of square errors shown in the table 4.1.

$$\rho(v_1) = p_4 v_1^4 + p_3 v_1^3 + p_2 v_1^2 + p_1 v_1 + p_0 \tag{4.1}$$

Table 4.1: Coefficients obtained for DPG(1) + H2O blends density, at 20 °C, polynomial fitting.

p_0	p_1	p_2	p_3	p_4	SSE_ρ
2.953	-2.734	-17.490	12.970	1033	26.44

The resutls obtained are displayed in figure 4.3. It can be seen that the behavior of the liquid mixture deviates from the ideal, represented in the graph as the molar average of the property, measuring a non-linear increase with respect to the molar formulation with a density maximum when the mixture has 60% of DPG in volume.

4.3 Surface Tension

In total, 9 points per each measurement have been taken. The disposition of of the data is shown the figures 4.4 and 4.5.

Connors and Wright model, equation 2.7 has been chosen for the good results given in the chemical literature. In order to correlate the data, a linearization of the function has been perfomed. It is necessary to define who new quantities, the "reduced surface tension":

$$\sigma_* = \frac{\sigma_1 - \sigma}{\sigma_1 - \sigma_2} \tag{4.2}$$

And the quantity R:
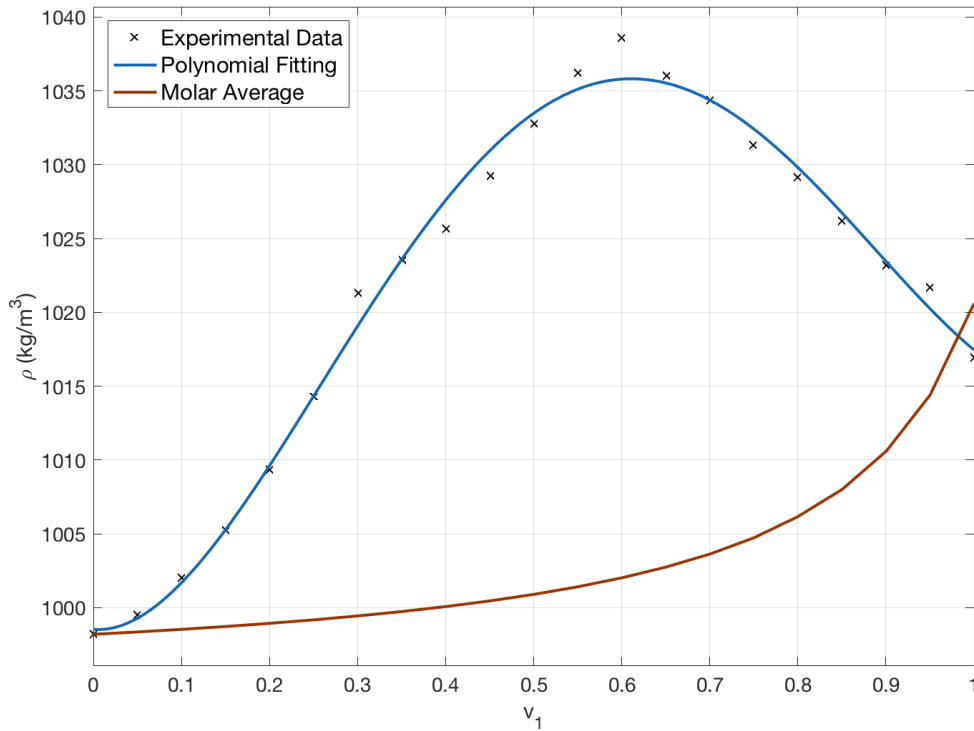
Figure 4.3: Experimental data, estimation and polynomial fitting of the different mixtures of DPG(1) + H2O(2) at 20 °C and different volume fractions.
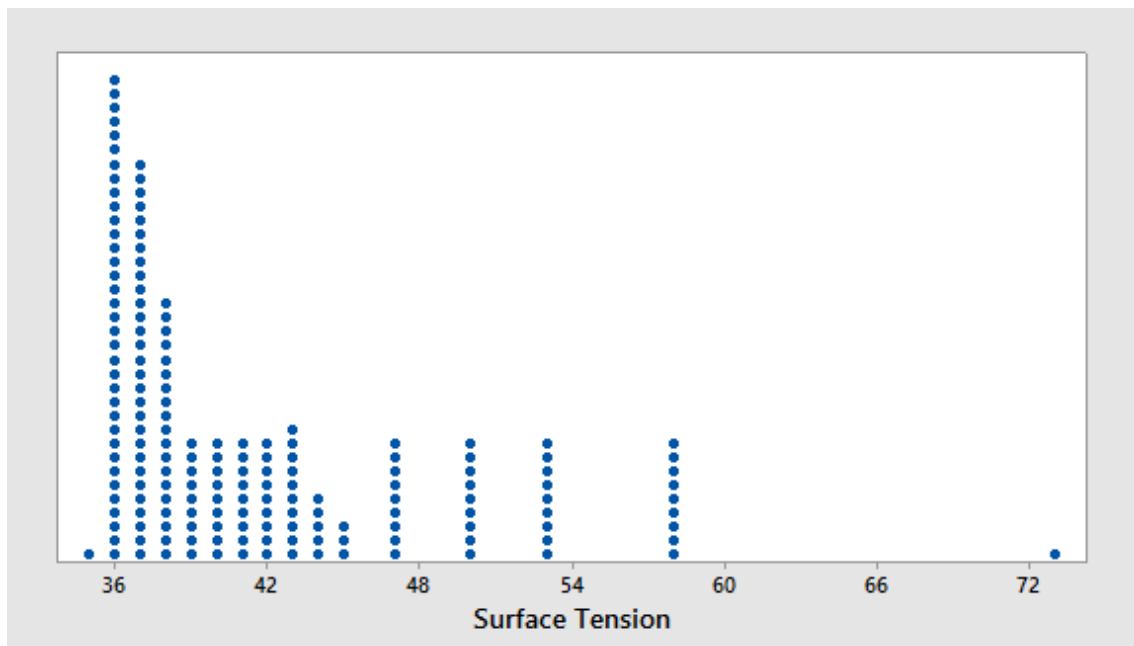
Figure 4.4: Surface tension experimental data distribution. One dot can represent up to 5 points.
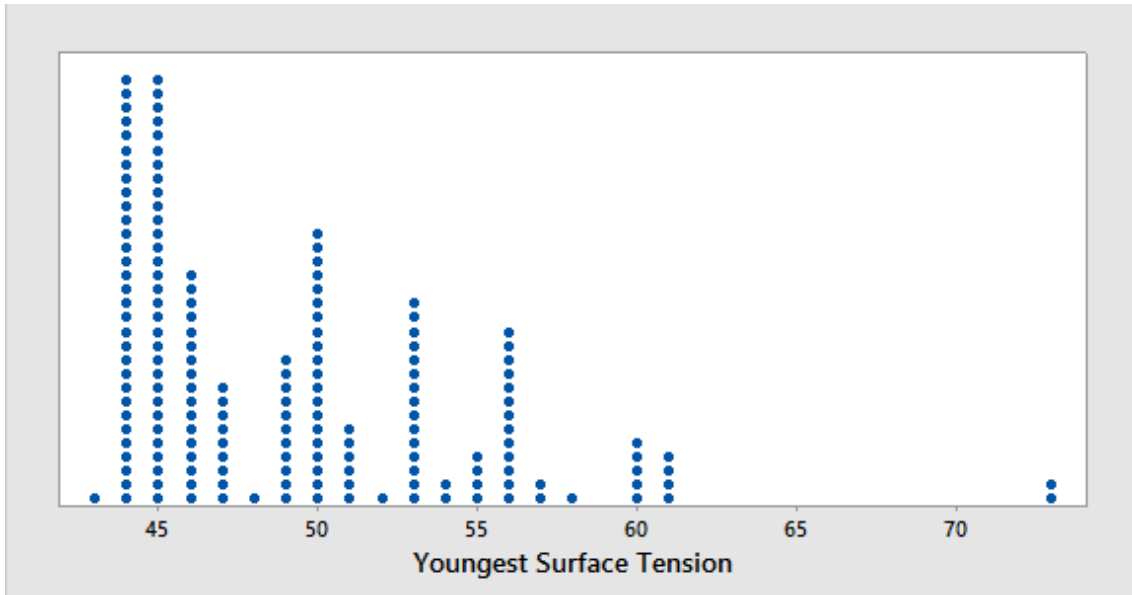
**Figure 4.5:** Youngest surface tension experimental data distribution. One dot can represent up to 5 points.

$$R = \frac{\sigma_*}{x_2} \tag{4.3}$$

So, the linearized version of the equation 2.7 is, equation 4.4. Plotting the quotient S and the DPG molar fraction, it is possible to obtain the parameters a and b can be seen in the figure 4.6, plus the coefficients and sum of square errors in the table 4.2.

$$S = \frac{x_1}{R-1} = \frac{1}{b} - \frac{ax_1}{b} \tag{4.4}$$

Table 4.2: Coefficients for CW model obtained for DPG(1) + H2O blends surface tension, at 20 °C.

a	b	SSE_σ
-113.6314	-108.5305	0.0014

As expected, the equilibrium surface tension values measured for the liquid mixtures are below the molar average. This can be appreciated in the figure 4.7, as well as in the figure 4.8, where all the values for the excess surface tension are negative.

The excess surface tension has been correlated by means of the Myers and Scott equation, 2.12. Here, we use a m of 5, making it a 10 adjustable parameters correlation. Equation 4.5 has been used for calculating the standard deviation. The results for the adjustable parameters and the standard deviation are listed in the table 4.3. The trend is plotted in figure 4.8.

$$SD_\sigma = \left[\frac{\sum(\Delta\sigma_{exp} - \Delta\sigma_{calc})}{n-p} \right]^{1/2} \tag{4.5}$$
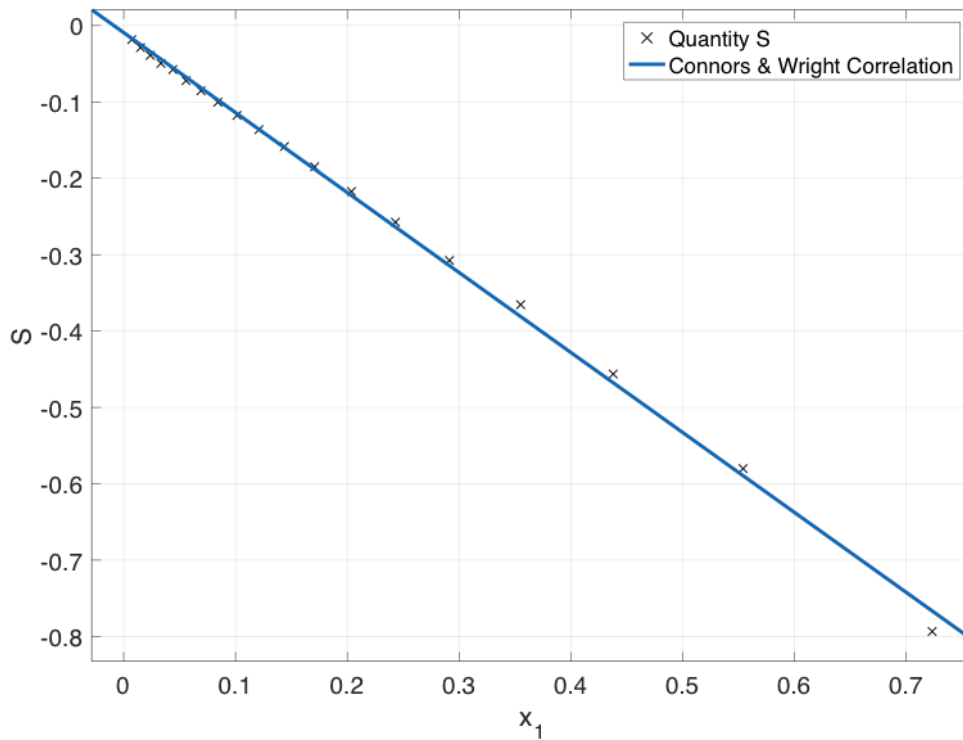
Figure 4.6: Plot of the quantity S vs the molar fraction.

Where n is the number of experimental points, and p is the number of parameters used in the correlation.

Table 4.3: Coefficients for MS correlation obtained for DPG(1) + H2O blends excess surface tension, at 20 °C.

B_0	B_1	B_2	B_3	B_4
1842.0	-291.7	-1982.0	249.3	104.6

C_0	C_1	C_2	C_3	C_4
-26.660	-22.780	27.320	22.210	-2.224

SD_σ				
0,3471				

Finally, figures 4.9 and 4.10 show the difference between the experimental data and the models used for the correlations. As can be seen in the figure 4.10, the average deviation for the CW model is 3.5%, and for the MS is below 1%. Taking into consideration that the MS model is computationally more complex, the deviation obtained are in line with expectations.
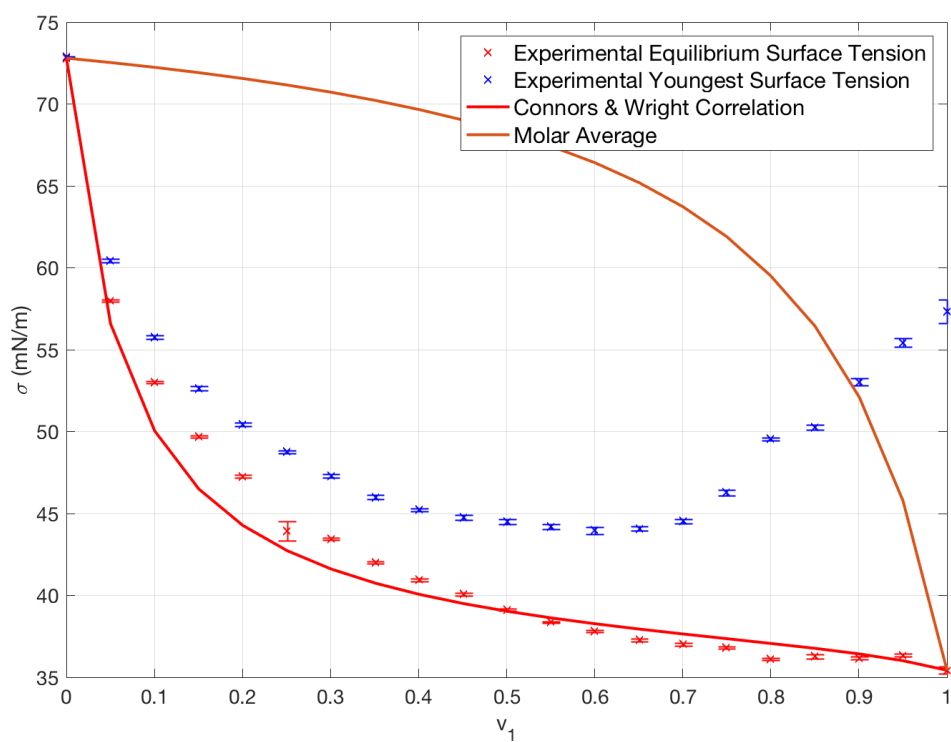
Figure 4.7: Experimental data error graph and CW correlation of the different mixtures of DPG(1) + H2O(2) at 20 °C and different volume fractions.
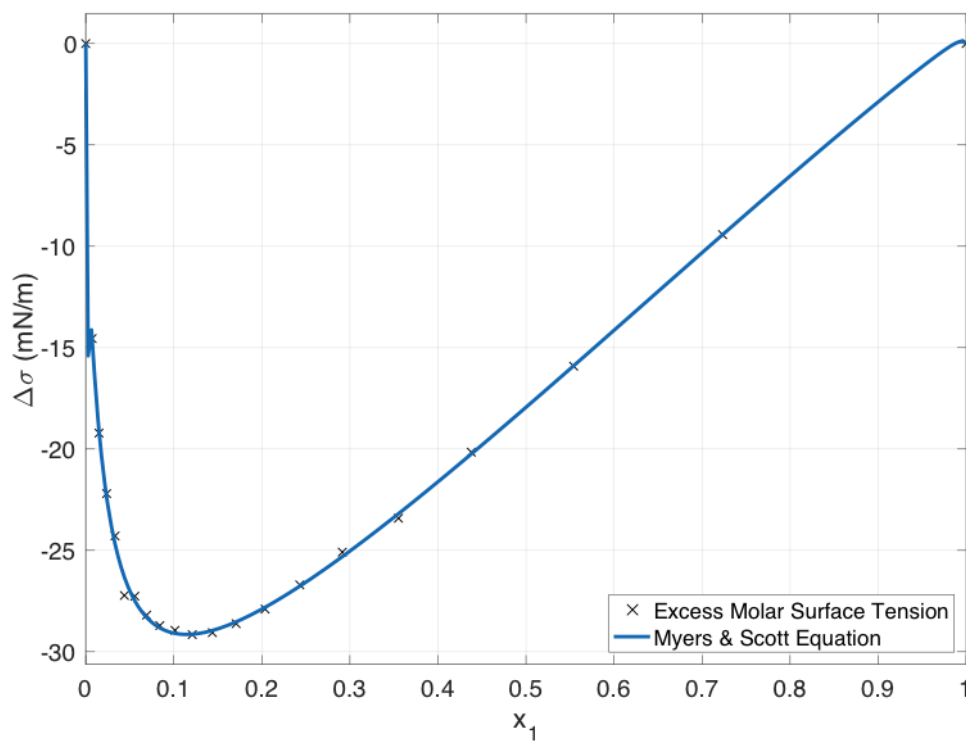
Figure 4.8: Excess surface tension and MS fitting of the different mixtures of DPG(1) + H2O(2) at 20 °C and different molar fractions.
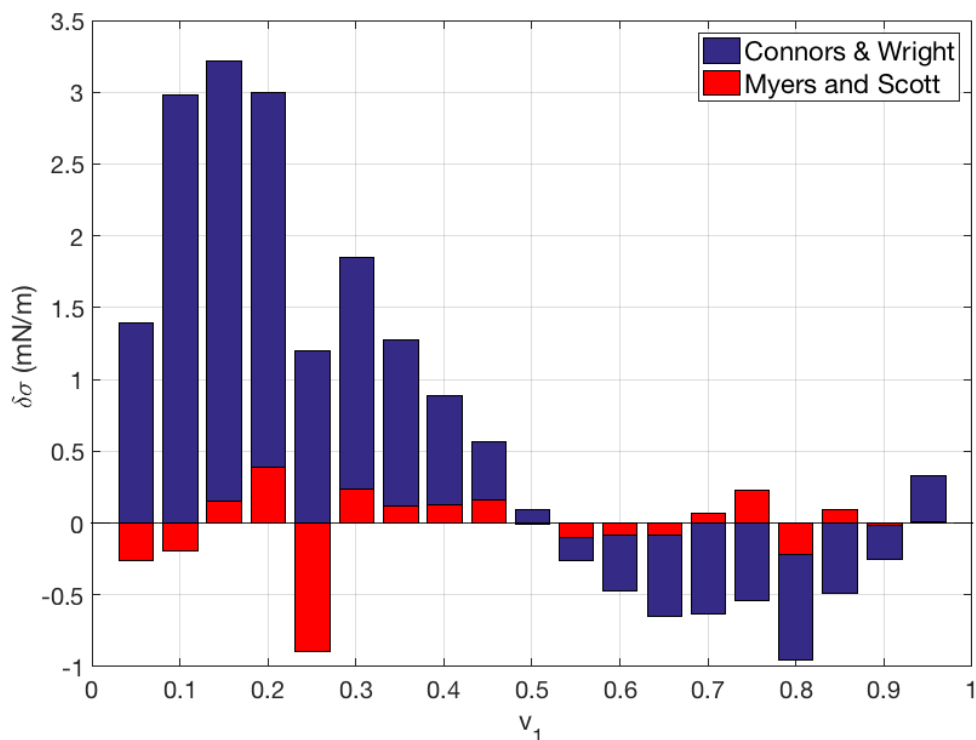
Figure 4.9: Difference between the experimental data and the estimated value using CW model, and MS equation.

4.4 Viscosity

As has been done for density and surface tension, viscosity data is an average of two runs of more than twenty points in order to be dona to obtain reasonable error. Figure 4.11 displays the data distribution for the viscosity data.

In that case, the results have been correlated using the TK equation, equation 2.23. Obtaining the results listed in the table 4.4. The sum of square errors obtained is high, but here it is important to note that the model is a three dimensional correlation. As can be seen in the figure 4.12, the model follows the data trend without problem. Also, the simpliest viscosity prediction, a molar average, has been found to be reasonably accurate.

Table 4.4: Coefficient for TK model obtained for DPG(1) + H2O blends viscosity, at 20 °C.

d	SSE_μ
14.15	157.00

Repeating the same procedure as for the surface tension, excess viscosity has been correlated with the RK equation, equation 2.28, giving the result plot in figure 4.13. The adjustable parameters and the standard deviation obtained for the model are listed in the following table 4.5.
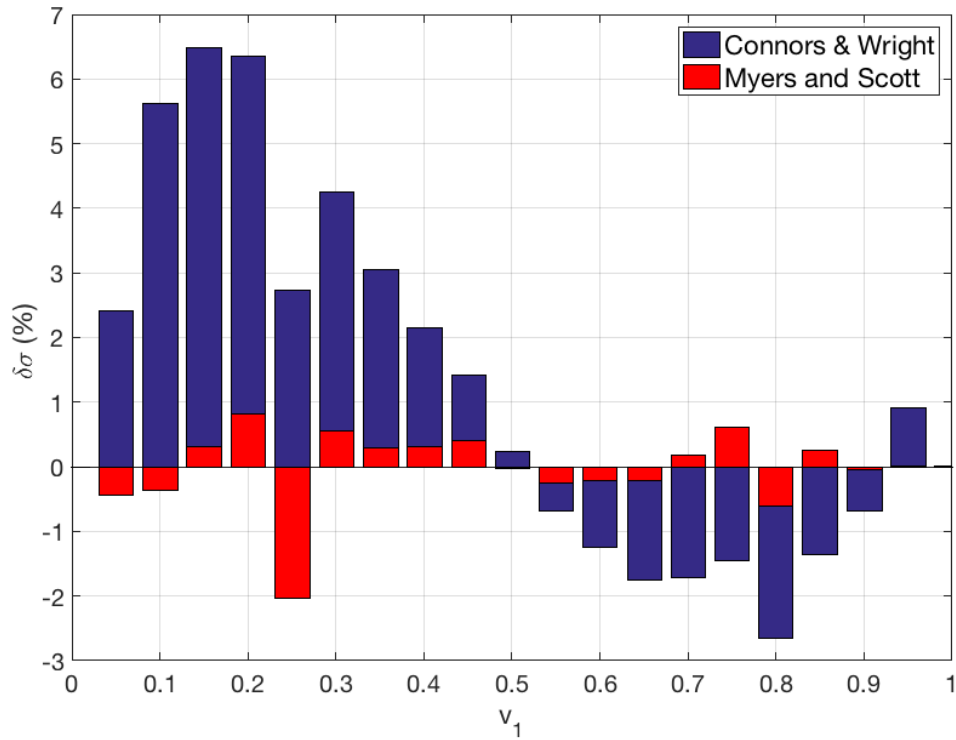
Figure 4.10: Relative difference between the experimental data and the estimated value using CW model, and MS equation.
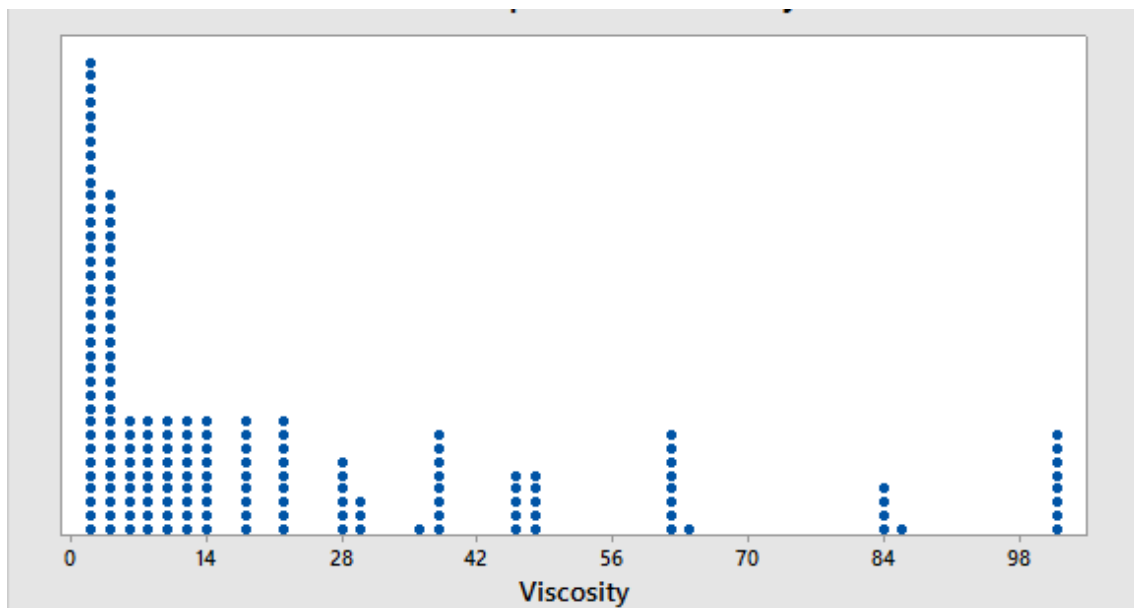
Figure 4.11: Viscosity experimental data distribution. One dot can represent up to 5 points.
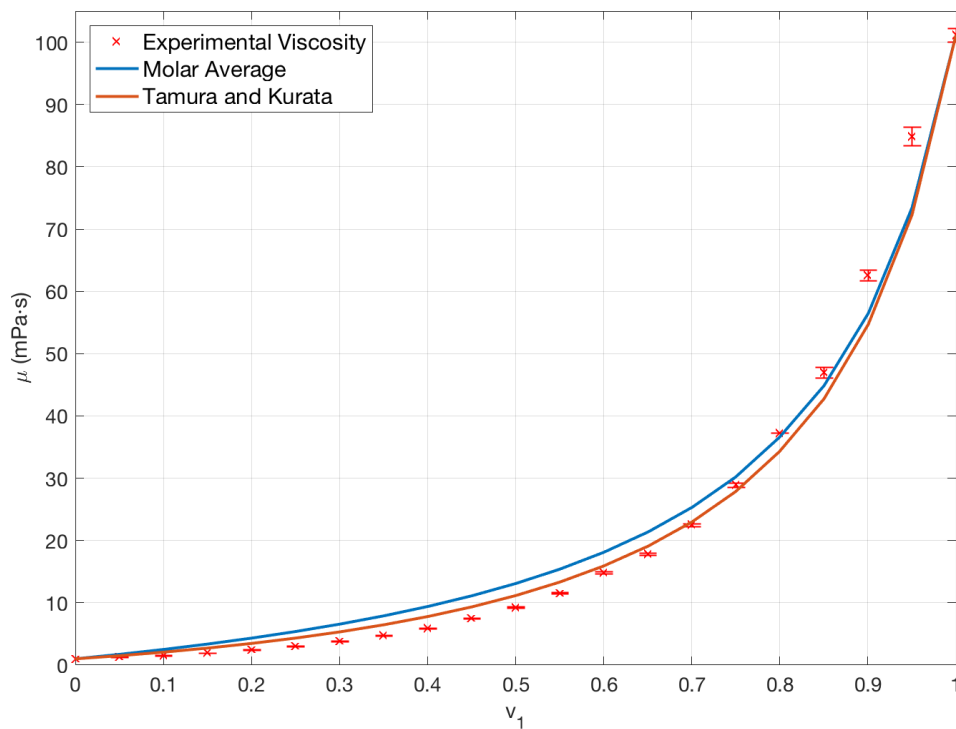
Figure 4.12: Prediction, Tamura and Kurata correlation, and error graph of the viscosity of DPG(1) + H2O(2) blends at 20 °C and different volume fractions.

Table 4.5: Parameters obtained for RK equation obtained for DPG(1) + H2O blends viscosity, at 20 °C.

A_0	A_1	A_2	A_3	A_4	SSE_μ
17.35	59.88	32.58	70.80	12.28	0.2196
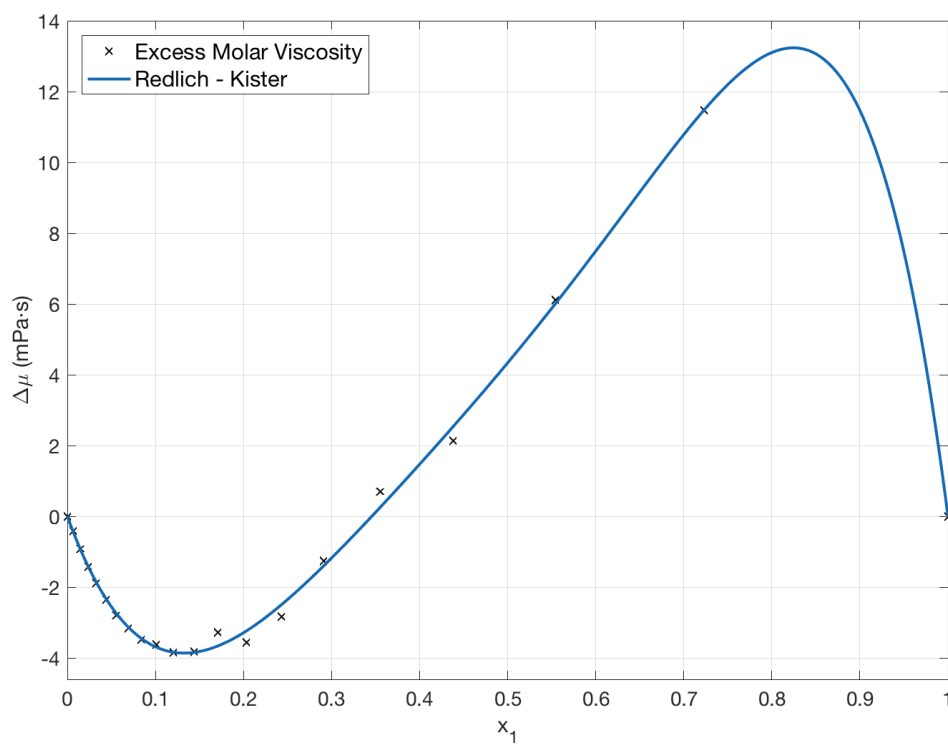
Figure 4.13: RK correlation for excess viscosity of the different mixtures of DPG(1) + H2O(2) at 20 °C and different molar fractions.

Lastly, as can be seen in the figure 4.14, there are some major differences when using the TK model. Even though the model follows the data trend, the deviation in viscosity maybe low in some cases. In the figure 4.15 is shown that the discrepancies are up to 42% in some instances. On the other hand, the RK equation gives accuracies below 3% except for really low DPG volume fractions.
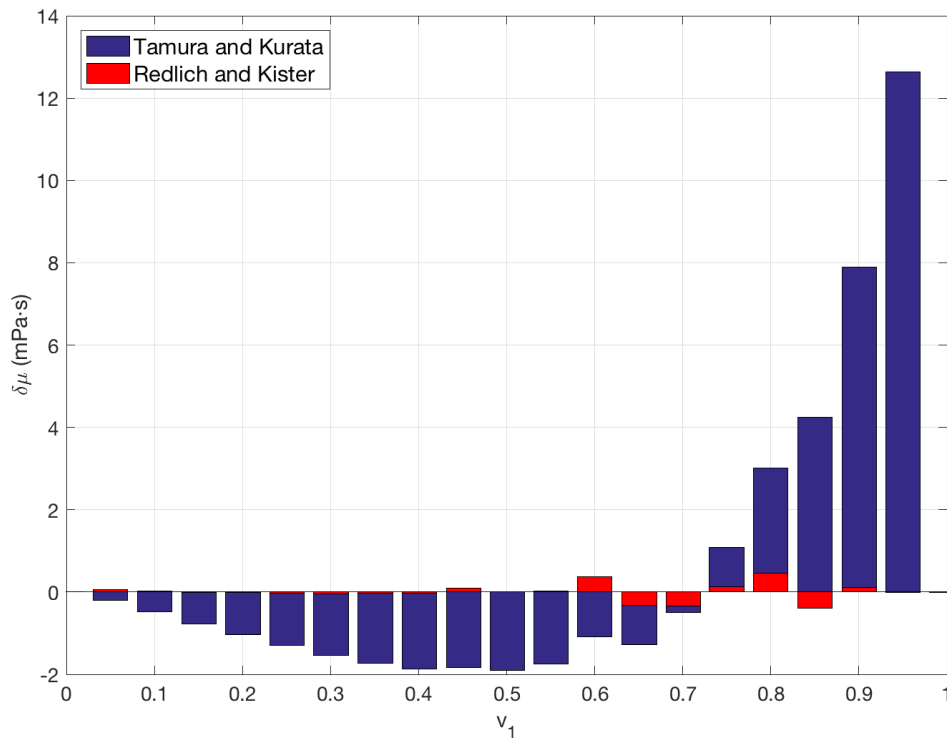
**Figure 4.14:** Difference between the experimental data and the estimated value using TK model, and RK equation.
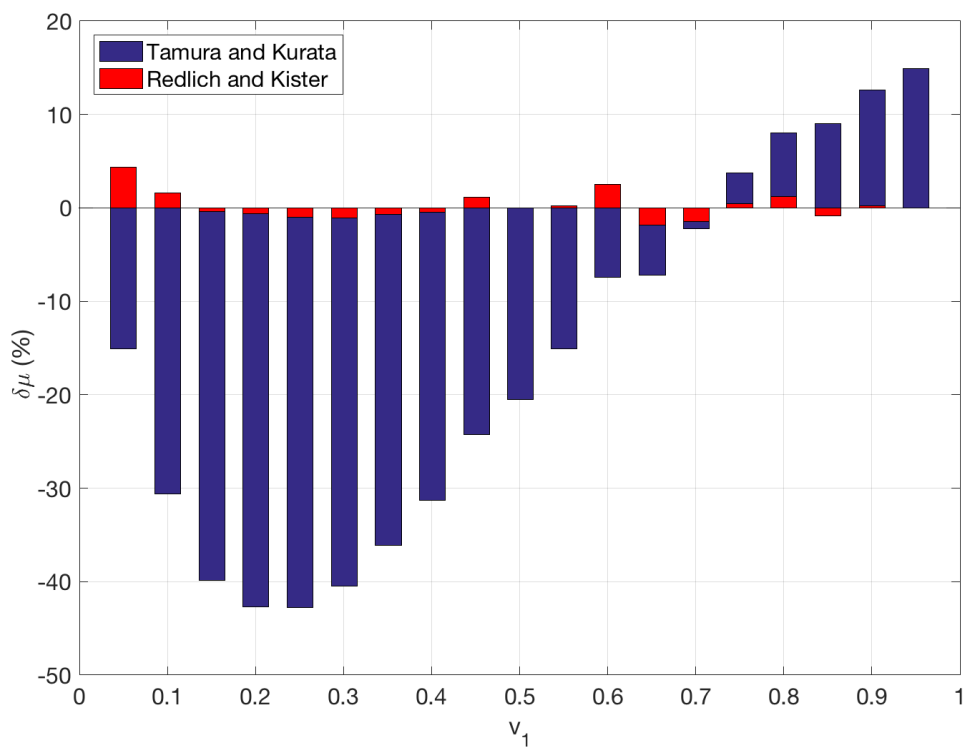
Figure 4.15: Relative difference between the experimental data and the estimated value using TK model, and RK equation.

5 Conclusion

From the begining, the main goal of the project was to obtain curves for three different fluid properties: density, surface tension and viscosity, and verify the data trend by means of empirical or theoretical parameter models.

First of all, the prepared blends have low uncertanties and are considered to be accurate. Uncertainties below 1% and a difference between the theoretical and real volume fraction have been achieved.

Second of all, it has been observed a non linear behavior for the density, as expected for real mixtures. Also, as the literature says, a negative excess surface tension has been obtained for the different blends.

Third of all, the tested empirical equations correlate with good results the experimental data for the three fluid properties. As for the comparison of the models, it has obtained far better results with the models using molar excess properties. Nevertheless, all the models follow the experimental data trend.

Finally, the uncertainties for all the measurements are low except for the density experiment, where it has not been calculated because the data is not statiscally relevant. Besides that, it is good enough to have an idea of how the dipropylene glycol and water density behaves once they are blended, in addition to a good estimation of the its value.

5.1 Future targets

The future targets proposed for continuing the present project are the following:

1. Extense study of the mixtures density.

2. Refractive index tracking of the blends.

3. Tertiary blend with another high refractive index fluid.

4. Obtention of the blend properties with fluorescent particles.

5. Conclusion

Bibliography

[1] Amir Abbas Rafati, Ahmad Bagheri, and Mojgan Najafi. Experimental data and correlation of surface tensions of the binary and ternary systems of water + acetonitrile + 2-propanol at 298.15 k and atmospheric pressure. *Journal of Chemical & Engineering Data*, 55(9):4039–4043, 2010. doi: 10.1021/je1001329.

[2] HU Yongqi; LI Zhibao; LU Jiufang; LI Yigui; JIN Yong. A new model for the surface tension of binary and ternary liquid mixtures based on peng- robinson equation of state. *Chinese Journal of Chemical Engineering*, 5(3):193–199, 1997.

[3] Joel Escobedo and G. Ali Mansoori. Surface tension prediction for liquid mixures. *AlChE Journal*, 44(10):2324–2332, 1998. doi: 10.1002/aic.690441021.

[4] Kim SW, Jhon MS, Ree T, and Eyring H. The surface tension of binary liquid mixtures. *Proceedings of the National Academy of Sciences of the United States of America*, 59(2):336–342, 1968.

[5] J. G. Eberhart. The surface tension of binary liquid mixtures. *The Journal of Physical Chemistry*, 70(4):1183–1186, 1966. doi: 10.1021/j100876a035.

[6] EXNER O. Conception and significance of the parachor. *Nature*, 196(4857): 890–891, 1962.

[7] Kenneth A. Connors and James L. Wright. Dependence of surface tension on composition of binary aqueous-organic solutions. *Analytical Chemistry*, 61(3): 194–198, 1989. doi: 10.1021/ac00178a001.

[8] Saeid Azizian, , and Maryam Hemmati. Surface tension of binary mixtures of ethanol + ethylene glycol from 20 to 50 Â°c. *Journal of Chemical & Engineering Data*, 48(3):662–663, 2003. doi: 10.1021/je025639s.

[9] Fu Jufu, Li Buqiang, and Wang Zihao. Estimation of fluid-fluid interfacial tensions of multicomponent mixtures. *Chemical Engineering Science*, 41(10):2673 – 2679, 1986. ISSN 0009-2509. doi: http://dx.doi.org/10.1016/0009-2509(86) 80055-0.

[10] Laura Mosteiro, Alejandra B. Mariano, L. M. Casás, Manuel M. Piñeiro, and José L. Legido. Analysis of surface tension, density, and speed of sound for the ternary mixture dimethyl carbonate + p-xylene + n-octane. *Journal of Chemical & Engineering Data*, 54(3):1056–1062, 2009. doi: 10.1021/je800594e.

[11] B.M.S Santos, A.G.M Ferreira, and I.M.A Fonseca. Surface and interfacial tensions of the systems water + n-butyl acetate + methanol and water + n-pentyl acetate + methanol at 303.15 k. *Fluid Phase Equilibria*, 208(102):1 – 21, 2003. doi: http://dx.doi.org/10.1016/S0378-3812(02)00320-5.

[12] Donald B. Myers and Robert L. Scott. Thermodynamic functions for nonelec-

trolyte solutions. *Industrial & Engineering Chemistry*, 55(7):43–46, 1963. doi: 10.1021/ie50643a008.

[13] Dabir S. Viswanath, Tushar K. Ghosh, Dasika H. L. Prasad, Nidamarty V.K. Dutt, and Kalipatnapu Y. Rani. *Viscosity of Liquids*. Springer Netherlands, 2007.

[14] Boris Zhmud. Viscosity blending equations. *LUBE: The European Lubricants Industry Magazine*, 93(121):22–27, 2014. doi: 10.1021/je990059p.

[15] Mikio Tamura and Michio Kurata. On the viscosity of binary mixture of liquids. *Bulletin of the Chemical Society of Japan*, 25(1):32–38, 1952. doi: DOI:10.1246/bcsj.25.32.

[16] Tongfan Sun, , and Amyn S. Teja. Density, viscosity and thermal conductivity of aqueous solutions of propylene glycol, dipropylene glycol, and tripropylene glycol between 290 k and 460 k. *Journal of Chemical & Engineering Data*, 49 (5):1311–1317, 2004. doi: 10.1021/je049960h.

[17] *A Guide to Glycols*, 2003.

[18] *Instruction Manual: FX/FY Series*, 1987.

[19] *Bubble Pressure Tensiometer - BP50*, 2015.

[20] *Brookfield DV2T Viscometer M13-167-B0614*, 2015.

A Auxiliar Calculations

The calculations perfomed to obtain the results shown in the tables B.1, B.2 and B.3 are explained in this chapter.

A.1 Balance Accuracy

In order to guarantee the quality of the experimental data, it is important to know the uncertainty introduced by the instruments used to measure. This can be calculated as the square sum of the systematic and random errors of the device:

$$e_x = \left(\sum_{i=1}^{n} b_i^2 + \sum_{j=1}^{m} u_j^2 \right) \tag{A.1}$$

Where e_x denotes the device error, b_i is the systematic error and u_j the random error.

For the balance FX-300 these are the errors introduced [18]:

1. The resolution of the device is $0.001\ g$, so:

$$u_{res} = \frac{Resolution}{2} = 0.0005\,g \tag{A.2}$$

2. Repeatability error:

$$u_{rep} = 0.001\,g \tag{A.3}$$

3. Linearity error:

$$u_{lin} = 0.002\,g \tag{A.4}$$

4. Sensitivity drift:

$$u_{S.drift}(T) = 3 \cdot 10^{-6}\,\frac{g}{°C} \tag{A.5}$$

   The temperature at the lab is 20 $°C$ so:

$$u_{S.drift} = 60 \cdot 10^{-6}\,g \tag{A.6}$$

Therefore, using the equation A.1 it is obtained:

$$e_{mass} = \left(u_{res}^2 + u_{rep}^2 + u_{lin}^2 + u_{S.drift}^2 \right)^{1/2} = 0.00229\,g \tag{A.7}$$

A.2 Volume

As said in the section 3.1, the blends have been prepared by mass, but the interest is to know the properties at different volume fraction at 20 °C. In order to do so, densities of pure liquids at 20 °C have been used to do the conversion, 2.1. Also, due to more information, a 1% density relative error has been asumed for the following calculations.

If the mass, m, and the density, ρ, are known, the volume can be calculated as:

$$V = \frac{m}{\rho} \tag{A.8}$$

The error associated with this conversion, e_V, can be determined by means of error propagation:

$$e_V = \sqrt{\left(\frac{\partial V}{\partial m}e_{mass}\right)^2 + \left(\frac{\partial V}{\partial \rho}e_\rho\right)^2} \tag{A.9}$$

Where e_ρ represents the density error.

Continuing with the calculation, the error associated to the volume can be obtained with the following expression:

$$e_V = \sqrt{\left(\frac{1}{\rho}e_{mass}\right)^2 + (me_\rho)^2} \tag{A.10}$$

A.3 Volume Fraction

Once the volume of both components has been calculated, it is possible to obtain the real volume fraction, v_i as:

$$v_i = \frac{V_i}{V_T} \tag{A.11}$$

Where V_i is the volume of the component i, and V_T represents the sum of components volume.
For a two liquids mixture:

$$v_i = \frac{V_i}{V_i + V_j} \tag{A.12}$$

Again, using error propagation it is possible to obtain the uncertainty associated to the volume fraction:

$$e_{v_i} = \sqrt{\left(\frac{\partial v_i}{\partial V_i}e_{V_i}\right)^2 + \left(\frac{\partial v_i}{\partial V_j}e_{V_j}\right)^2} \tag{A.13}$$

$$e_{v_i} = \sqrt{\left(\frac{V_j}{(V_i + V_j)^2}e_{V_i}\right)^2 + \left(\frac{V_i}{(V_i + V_j)^2}e_{V_j}\right)^2} \tag{A.14}$$

If $i = DPG$; and $j = H2O$:

$$e_{v_{DPG}} = \sqrt{\left(\frac{V_{H2O}}{(V_{DPG} + V_{H2O})^2}e_{V_{DPG}}\right)^2 + \left(\frac{V_{DPG}}{(V_{DPG} + V_{H2O})^2}e_{V_{H2O}}\right)^2} \tag{A.15}$$

And, if $i = H2O$; and $j = DPG$:

II

$$e_{v_{H2O}} = \sqrt{\left(\frac{V_{DPG}}{(V_{H2O} + V_{DPG})^2}e_{V_{H2O}}\right)^2 + \left(\frac{V_{H2O}}{(V_{H2O} + V_{DPG})^2}e_{V_{DPG}}\right)^2} \quad \text{(A.16)}$$

It is possible to conclude that the error for the DPG and the H2O is the same:

$$e_{v_{DPG}} = e_{v_{H2O}} \quad \text{(A.17)}$$

A.4 Molar Fraction

First of all, it is necessary to know the number of moles, χ, of the components in the mixture. To do that, the measured mass, m, is divided by the molar mass, M: It is possible to conclude that the error for the DPG and the H2O is the same:

$$\chi = \frac{m}{M} \quad \text{(A.18)}$$

Secondly, the molar fraction of a component, x_i, of a binary mixture is calculated as follows:

$$x_i = \frac{\chi_i}{\chi_i + \chi_j} \quad \text{(A.19)}$$

Third of all, the error in the number of moles has to be known. Assuming that the uncertainty in the molar mass is negligible, the uncertainty in the amount of moles of the components, e_{χ_i} can be obtained converting the error in mass, e_{mass} to moles:

$$e_{\chi_i} = e_{mass}\frac{1}{M_i} \quad \text{(A.20)}$$

Finally, using error propagation and thanks to the similarity of the molar fraction expression A.19 and the volume fraction equation A.12, the error in the molar fraction, e_{x_i} is equal for both components and has the next formula:

$$e_{x_{DPG}} = e_{x_{H2O}} = \sqrt{\left(\frac{\chi_{DPG}}{(\chi_{H2O} + \chi_{DPG})^2}e_{\chi_{H2O}}\right)^2 + \left(\frac{\chi_{H2O}}{(\chi_{H2O} + \chi_{DPG})^2}e_{\chi_{DPG}}\right)^2} \quad \text{(A.21)}$$

A.5 Uncertainty in Data

The error in data, is given by square root of the square sum two factors: measurement error and instrument accuracy:

$$e_{Data} = \sqrt{e_{device}^2 + e_{measure}^2} \quad \text{(A.22)}$$

The error measure, is an uncertainty associated with the dispersion of data regarding the same point. In that case, the points taken are less than 30, therefore, a t-Student distribution is used for the data treatment.

$$x = \bar{x} \pm e_{measure} = \bar{x} \pm t_{\nu,P(\%)}\frac{S_x}{\sqrt{N}} \quad \text{(A.23)}$$

Where x is the measure, $\bar{x}$ is the average value, S_x is the standard deviation of the measurements, N represents the number of point for a replica, $t_{\nu,P(\%)}$ represents the value of the t-Student distribution with ν degrees of freedom, and $P(\%)$ probability (it has been considered a 95% for all cases).

A. Auxiliar Calculations

B Experimetal Data

Table B.1: DPG (1) + H2O (2) blend composition at 20 °C.

Blend	DPG (g)	H2O (g)	DPG (cm^3)	H2O (cm^3)	DPG (mol)	H2O (mol)
1	0.000	0.000	0.000	0.000	1.000	0.000
2	194.512	9.990	190.586	10.008	0.723	0.277
3	184.141	19.894	180.424	19.930	0.554	0.446
4	173.910	29.969	170.400	30.023	0.438	0.562
5	163.685	40.139	160.381	40.211	0.354	0.646
6	153.446	50.098	150.349	50.188	0.291	0.709
7	143.219	59.868	140.328	59.976	0.243	0.757
8	132.993	69.793	130.309	69.919	0.204	0.796
9	122.749	80.008	120.271	80.152	0.171	0.829
10	112.534	89.966	110.263	90.128	0.144	0.856
11	102.303	99.815	100.238	99.995	0.121	0.879
12	92.074	109.609	90.216	109.807	0.101	0.899
13	81.836	119.548	80.184	119.764	0.084	0.916
14	71.615	129.489	70.170	129.723	0.069	0.931
15	61.384	139.610	60.145	139.862	0.056	0.944
16	51.155	149.518	50.122	149.788	0.044	0.956
17	40.919	159.588	40.093	159.876	0.033	0.967
18	30.693	169.481	30.073	169.787	0.024	0.976
19	20.461	179.574	20.048	179.898	0.015	0.985
20	10.233	189.433	10.026	189.775	0.007	0.993
21	0.000	0.000	0.000	0.000	0.000	1.000

Table B.2: DPG (1) + H2O (2) blend volume and molar fraction composition at 20 °C.

Blend	v_{1T}	v_{2T}	v_1	v_2	δv (%)	x_1	x_2	δx (%)
1	100.00	0.00	100.00	0.00	0.00	100.00	0.00	0.00000
2	95.00	5.00	95.01	4.99	0.07	72.33	27.67	0.00459
3	90.00	10.00	90.05	9.95	0.13	55.41	44.59	0.00286
4	85.00	15.00	85.02	14.98	0.18	43.79	56.21	0.00191
5	80.00	20.00	79.95	20.05	0.23	35.38	64.62	0.00134
6	75.00	25.00	74.97	25.03	0.27	29.14	70.86	0.00099
7	70.00	30.00	70.06	29.94	0.30	24.31	75.69	0.00076
8	65.00	35.00	65.08	34.92	0.33	20.37	79.63	0.00060
9	60.00	40.00	60.01	39.99	0.35	17.08	82.92	0.00048
10	55.00	45.00	55.02	44.98	0.36	14.38	85.62	0.00040
11	50.00	50.00	50.06	49.94	0.36	12.10	87.90	0.00034
12	45.00	55.00	45.10	54.90	0.36	10.14	89.86	0.00030
13	40.00	60.00	40.10	59.90	0.35	8.42	91.58	0.00026
14	35.00	65.00	35.10	64.90	0.33	6.91	93.09	0.00024
15	30.00	70.00	30.07	69.93	0.30	5.57	94.43	0.00021
16	25.00	75.00	25.07	74.93	0.27	4.39	95.61	0.00020
17	20.00	80.00	20.05	79.95	0.23	3.33	96.67	0.00019
18	15.00	85.00	15.05	84.95	0.18	2.37	97.63	0.00018
19	10.00	90.00	10.03	89.97	0.13	1.51	98.49	0.00017
20	5.00	95.00	5.02	94.98	0.07	0.72	99.28	0.00016
21	0.00	100.00	0.00	100.00	0.00	0.00	100.00	0.00000

Table B.3: Averaged studied fluid properties for DPG (1) + H2O (2) blends at 20 °C and different volume fractions.

v_1	$\rho \left(\dfrac{kg}{m^3}\right)$	$\mu \ (mPa \cdot s)$	$\delta\mu \ (\%)$	$\sigma \left(\dfrac{mN}{m}\right)$	$\delta\sigma \ (\%)$	$\sigma_Y \left(\dfrac{mN}{m}\right)$	$\delta\sigma_Y \ (\%)$
1.00	1,016.964	101.140	1.050	35.430	0.570	57.330	1.230
0.95	1,021.704	84.910	1.770	36.340	0.240	55.430	0.470
0.90	1,023.195	62.610	1.380	36.180	0.200	53.030	0.430
0.85	1,026.177	47.000	1.840	36.280	0.350	50.280	0.300
0.80	1,029.156	37.280	0.010	36.110	0.190	49.540	0.210
0.75	1,031.306	28.930	1.220	36.820	0.160	46.280	0.390
0.70	1,034.357	22.520	1.070	37.010	0.190	44.520	0.260
0.65	1,036.007	17.840	1.010	37.290	0.240	44.080	0.310
0.60	1,038.604	14.820	1.220	37.800	0.180	43.970	0.510
0.55	1,036.229	11.580	1.140	38.370	0.150	44.210	0.350
0.50	1,032.804	9.280	1.130	39.120	0.170	44.500	0.340
0.45	1,029.261	7.540	1.040	40.070	0.240	44.760	0.310
0.40	1,025.649	5.950	1.110	40.940	0.240	45.220	0.160
0.35	1,023.547	4.760	1.230	42.020	0.160	46.000	0.270
0.30	1,021.288	3.800	1.440	43.460	0.140	47.280	0.220
0.25	1,014.264	3.040	1.470	43.930	1.370	48.760	0.210
0.20	1,009.342	2.440	1.660	47.270	0.160	50.420	0.220
0.15	1,005.217	1.950	2.570	49.710	0.130	52.630	0.270
0.10	1,002.050	1.590	3.020	53.020	0.110	55.770	0.200
0.05	999.518	1.310	3.840	57.980	0.130	60.430	0.150
0.00	998.200	1.000	0.000	72.800	0.570	72.900	0.000